UCID - 16719

LAWRENCE LIVERMORE LABORATORY

University of California/Livermore, California

ROCK MODELING IN TENSOR74, A TWO-DIMENSIONAL LAGRANGIAN SHOCK PROPAGATION CODE

Donald E. Burton

John F. Schatz

March 19, 1975

Prepared for U. S. Atomic Energy Commission under contract no. W-7405-Eng-48

CONTENTS

ROCK MODELING IN TENSOR74, A TWO-DIMENSIONAL LAGRANGIAN SHOCK PROPAGATION CODE

ABSTRACT

TENSOR74 is a major revision of TENSOR, a computer code designed to solve stress wave propagation problems in two dimensions. The major physics modifications in TENSOR74 are in the area of constitutive modeling of solid materials. The new models, which are described in detail, take into account pore collapse, ductile and strain softening brittle failure, as well as tensile failure with void opening and closure. In addition, a modified form of linear artificial viscosity is described.

INTRODUCTION

TENSOR74 is a major modification of the TENSOR code which was originally conceived and written by Maechen and Sack[1] and later adapted by Cherry.[2] TENSOR74 provides numerical solutions to problems involving the propagation of stress waves in two dimensions. The code is a Lagrangian, explicit finite difference, continuum mechanics code which can take into account highly nonlinear material behavior.

This report gives a brief overview of the continuum mechanics equations which are solved and describes in detail the rock mechanics model used in TENSOR74. The finite difference equivalent for the differential continuum mechanics equations has been treated in considerable detail by others[1,2] and is not discussed here. The rock mechanics model is a two-dimensional version of a model formulated by J. Schatz for SOC73, the one-dimensional companion code of TENSOR74. General discussion of the philosophy of constitutive modeling used in both TENSOR74 and SOC73 may be found in Ref. 3.

As a convenience to code users, Table 1 lists the relationships between the notation used herein and code variables and input parameters.

SOLUTION OF THE INCREMENTALLY ELASTIC PROBLEM

During each code cycle, stress loading is treated initially as an incrementally elastic or "hypoelastic"[4] process which can be described by two independent elastic moduli over the range of stresses encountered during a single time step. The calculated stresses are later adjusted, if necessary, to take into account any inelastic behavior as described by the constitutive model.

The detailed finite difference solution to the incrementally elastic problem has been discussed in considerable detail elsewhere,[1,2] so only a brief outline of the

Table 1. Relationship between notation and code variables or mnemonics.

Material Parameters		TENSOR Grid Variables		Additional TENPLT Mnemonics		Additional TENSOR Output Names	
Card 24 Position	Notation	Variable	Notation	Mnemonic	Notation	Heading	Notation
1	ρ_0	U	u_r	RØ	r_0	MU MAX	ζ_m
2	c_0	V	u_z	ZØ	z_0	ANG	ψ
3	+V or $-v_0$	R	r	RHO	$\sqrt{r^2 + z^2}$	T1	T_1
4	T_0	Z	z	RHOA	$\mathrm{Tan}^{-1}(z/r)$	T2	T_2
5	Material number	DM, VN	Volume change × 3/π	SP	$\sqrt{u_r^2 + u_z^2}$	T3	T_3
6	C_1	Q	Q	SPA	$\mathrm{Tan}^{-1}(u_z/u_r)$	DEL R	$\Delta r = r - r_0$
7	+N or $-C_4$	L	L	CURLV	$\nabla \times \underline{u}$	DEL Z	$\Delta Z = z - z_0$
8	Number of $\zeta_A(P)$ table	P	P	DIVV	$\nabla \cdot \underline{u}$	QY	Equivalent of Y for Q tensor
9	Number of $\zeta_B(P)$ table	VZ	Initial volume × 3/π	CURLD	$\nabla \times \Delta \underline{r}$		
10	Number of gas table $\zeta_C(P)$	AM	Mass × 3/π	I2D	I_{2D}		
11	A_1	SDSP	c	I3D	I_{3D}		
12	A_2	AM	Zone area × 2	Y	Y		
13	A_3	TILQ	HE lighting time + bits	PBAR	$\bar{P}$		
14	E_f	TR	S_r	MU	ζ		
15	–	TZ	S_z	DEN	ρ		
16	–	TRZ	$S_{rz} = T_{rz}$	COMP	$\zeta + 1$		
17	ζ_3	Q	Q_r	MAT	Material number		
18	ζ_1	QZ	Q_z	EOS	Material state		
19	ζ_2	QRZ	Q_{rz}	TRR	T_r		
20	C_3	SSL	Overburden pressure + bits	TZZ	T_z		
21	$\bar{P}_{BD}$	SVI	s	TPP	T_ϕ		
22	–	CONE	P_v	TP	S_ϕ		
23	Number of $K_v(\bar{P})$ table	DV0	Initial compression	SIG1	T_1		
24	ζ_B	XMUS	ζ_m	SIG2	T_2		
25	Number $k_f(\bar{P})$ table	RU	$\Delta r = r - r_0$	SIG3	T_3		
26	C_2	ZU	$\Delta z = z - z_0$	SIGA	ψ		
27	–			P*Q	P*Q		
28	Overburden constant			KED	Kinetic energy density		
29	Overburden constant			IED	Internal energy density		
30	–			TED	Total energy density		
				KEN	Specific kinetic energy		
				IEN	Specific internal energy		
				TEN	Specific total energy		

solution will be presented. Although TENSOR74 can be used in either plane or cylindrical coordinates (r, z, ϕ), the latter mode is most often used and, consequently, will be the one described here. The region to be described in the calculation is discretized into a large number of quadrilateral zones in the r-z plane, the z-axis being the symmetry axis. The state of the material within each zone is described by a stress tensor ($\underline{\underline{T}}$) and a strain tensor ($\underline{\underline{\varepsilon}}$) which are both separated into their isotropic (P and Θ) and deviatoric ($\underline{\underline{S}}$ and $\underline{\underline{e}}$) components:

$$\begin{bmatrix} T_r & T_{rz} & 0 \\ T_{rz} & T_z & 0 \\ 0 & 0 & T_\phi \end{bmatrix} = -P\underline{\underline{I}} + \begin{bmatrix} S_r & S_{rz} & 0 \\ S_{rz} & S_z & 0 \\ 0 & 0 & S_\phi \end{bmatrix}$$

$$\begin{bmatrix} \varepsilon_r & \varepsilon_{rz} & 0 \\ \varepsilon_{rz} & \varepsilon_z & 0 \\ 0 & 0 & \varepsilon_\phi \end{bmatrix} = \frac{\Theta}{3}\underline{\underline{I}} + \begin{bmatrix} e_r & e_{rz} & 0 \\ e_{rz} & e_z & 0 \\ 0 & 0 & e_\phi \end{bmatrix} \qquad (1)$$

where $\underline{\underline{I}}$ is the identity tensor. The pressure or mean stress P and the volumetric strain Θ are then given by

$$P = -\frac{1}{3}(T_r + T_z + T_\phi)$$

$$\Theta = \varepsilon_r + \varepsilon_z + \varepsilon_\phi \ . \qquad (2)$$

The introduction of the first invariant quantities, P and Θ, allows the ϕ components to be carried implicitly in the solution. The off-diagonal components, T_{rz} and S_{rz}, are of course identical, as are ε_{rz} and e_{rz}.

The calculational procedure followed in a given zone during each cycle is shown in Fig. 1. In terms of P and the deviatoric stresses, the conservation laws reduce to the coupled equations of motion,

$$\rho\dot{u}_r = -\frac{\partial}{\partial r}(P - S_r) + \frac{\partial}{\partial z}S_{rz} + \frac{1}{r}(2S_r + S_z) + \rho g_r$$

$$\rho\dot{u}_z = -\frac{\partial}{\partial z}(P - S_z) + \frac{\partial}{\partial r}S_{rz} + \frac{1}{r}S_{rz} + \rho g_z \ , \qquad (3)$$

where u is the velocity, ρ is the density, and g is the gravitational body acceleration. The dissipative viscosity terms which are added to each of the stresses to smooth the sharp discontinuities characteristic of shock phenomena are not shown in the above equations. It is the user's option to include the gravitational terms. When they are included, each zone is given an initial pressure in an effort to partially balance the

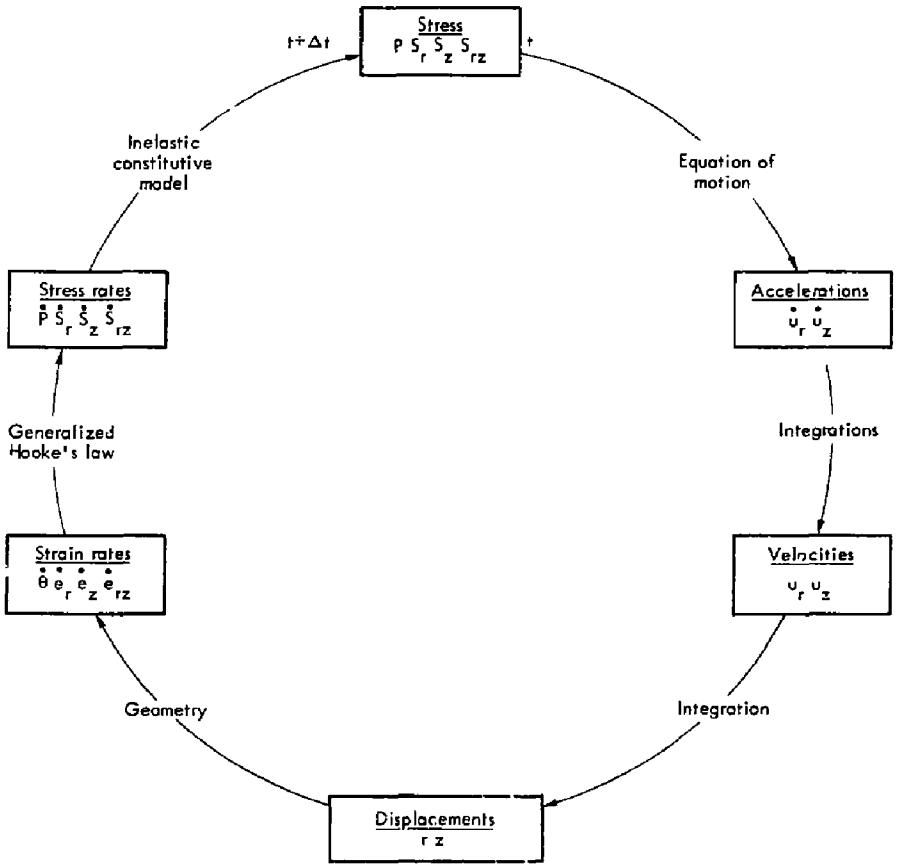

Fig. 1. Calculational cycle.

equations of motion to produce an initial equilibrium. While this procedure is incomplete because the deviators are not also initialized, it is probably adequate for many problems.

The accelerations are then integrated to yield the velocities, u_r and u_z, and the new coordinates, r and z. From geometrical considerations, the strain rates can then be calculated as

$$\dot{\theta} = \frac{\partial}{\partial r} u_r + \frac{\partial}{\partial z} u_z + \frac{u_r}{r}$$

$$\dot{\epsilon}_r = \frac{1}{3}\left(2\frac{\partial}{\partial r} u_r - \frac{\partial}{\partial z} u_z - \frac{u_r}{r}\right)$$

$$\dot{\epsilon}_z = \frac{1}{3}\left(2\frac{\partial}{\partial z} u_z - \frac{\partial}{\partial r} u_r - \frac{u_r}{r}\right)$$

$$\dot{\epsilon}_{rz} = \frac{1}{2}\left(\frac{\partial}{\partial z} u_r + \frac{\partial}{\partial r} u_z\right) . \qquad (4)$$

The resulting strain rates are then used to calculate the elastic stress rates using a generalization of Hooke's law that assumes the material is describable by an elastic bulk modulus k and an elastic shear modulus μ which are characteristic of the current state of the material. This is a "variable modulus" model in that it assumes a pressure dependent k and a similar dependence in μ if a constant Poisson's ratio (ν) is assigned. This arises through the relationship from linear elasticity,

$$\mu(k,\nu) = \frac{3k}{2}\left(\frac{1 - 2\nu}{1 + \nu}\right) .$$

In addition, the bulk modulus may also depend on the previous state of the material, as discussed below. The isotropic and deviatoric stress rates are then given by,

$$\dot{P} = -k\dot{\theta}$$

$$\dot{S}_r = 2\mu\dot{\epsilon}_r + 2S_{rz}\omega_{rz}$$

$$\dot{S}_z = 2\mu\dot{\epsilon}_z - 2S_{rz}\omega_{rz}$$

$$\dot{S}_{rz} = 2\mu\dot{\epsilon}_{rz} + (S_z - S_r)\omega_{rz} , \qquad (5)$$

where the factor

$$\omega_{rz} = 1/2\left(\frac{\partial u_r}{\partial z} - \frac{\partial u_z}{\partial r}\right)$$

is an angular velocity which corrects for the rigid body motion of the zone during the time step. The finite difference equations actually used in the code carry an additional higher order rotation term not shown in the above differential equations.[5]

Equations (5) apply to solid materials which are capable of supporting shear stress. The relevant expressions for fluids are obtained as a special case by setting the shear modulus to zero. The modeling of gradual phase transitions between the solid and fluid state is achieved through the artifice of using an effective shear modulus*

$$\mu = \mu_0 \left(1 - \frac{E}{E_f}\right),$$

where μ_0 is the shear modulus for the solid, E_f is the specific internal energy of fusion, and E is the current specific internal energy.

The next section discusses the model assumed in determining the bulk modulus and therefore the pressure integration. A later section discusses the integration and modification of the deviatoric equations.

PRESSURE INTEGRATION

In general, the pressure will be a function of both internal energy and specific volume; and several fluid models in TENSOR74 take this dependence into account. The pressure in solid rock, however, is assumed to have no dependence on internal energy. The model used in determining the effective bulk modulus for earth materials is intended to take into account two specific effects. The first is the permanent loss of porosity which occurs as the strength of the material bonds is exceeded.[6] The second is the void volume which is produced concomitant to tensile failure.

A given material is assumed to be describable in terms of two pressure-volume relationships, such as those labeled A and B in Fig. 2. These relations are given to the code as tables of pressure versus the excess compression ζ,† which is defined as

$$\zeta(P) = \frac{\rho}{\rho_0} \Theta$$

$$= \frac{\rho(P)}{\rho_0} - 1 \qquad (6)$$

---

*This effective modulus is to be used in all expressions in this report except those defining the damage parameter ϵ, Equations (20) and (24).

†The traditional notation, μ or mu, has been discarded in favor of ζ to avoid possible confusion with the shear modulus μ.

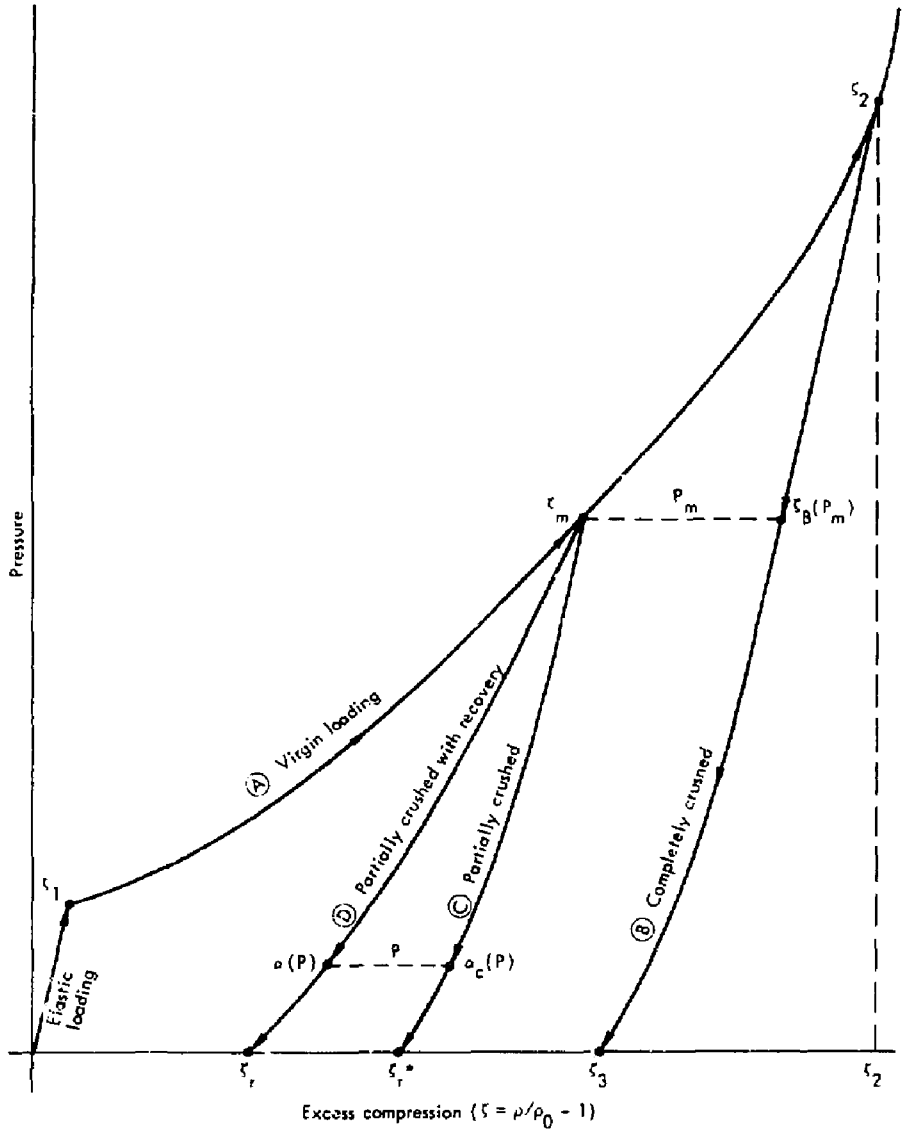

Fig. 2. Pressure-volume model.

where V_0 is the specific volume at $P = 0$. In these terms, the bulk modulus is given by

$$k(P) = \frac{\rho}{\rho_0} \frac{\partial P}{\partial \zeta}$$

$$= \frac{\rho}{\rho_0} \alpha \ , \tag{7}$$

where α is the slope of the current trajectory in P-ζ space.

The prescription followed in determining α, and therefore k, is illustrated in Fig. 2. The material is taken to load along a path termed the virgin loading path (A). The subsequent unloading behavior depends on the maximum compression ζ_m experienced by the material relative to two experimental points ζ_1 and ζ_2. If ζ_m has not exceeded ζ_1, then no permanent compaction can take place because the internal stresses have not exceeded the pore wall strength and allowed pore collapse to occur.* If the maximum compression ζ_m has exceeded ζ_2, then all pores have presumably collapsed; and the material must unload along the path B for completely crushed material. In principle, the crushed path would be the loading and unloading path for pure nonporous matrix material. The intercept ζ_3 is the maximum permanent compaction and is approximately equal to the gas-filled porosity of the material.

When ζ_m is greater than ζ_1 but does not yet exceed ζ_2, then the material is only partially compacted and must unload along a path between the crushed and virgin loading curves. If the partial pore collapse were permanent, the appropriate unloading path would have to be consistent with the unloading behavior of the fully crushed matrix material. That is to say, partially crushed material would have to unload along path C in Fig. 2, which is parallel to the crushed path B and will intersect the ζ axis at ζ_r^*,

$$\zeta_r^*(\zeta_m) = \zeta_3 - (\zeta_B - \zeta_m) \ .$$

However, partially compacted material usually exhibits elastic recovery of some porosity, presumably because many of the pore walls have not been stressed to failure. This means that the material must unload along some path D which lies to the left of C. The specification of this path is accomplished as follows. The residual porosity, which is the intercept ζ_r of D with the ζ axis, can be deduced from laboratory data and expressed as a polynomial,

$$\zeta_r(\zeta_m) = \zeta_3\left(A_1 s + A_2 x^2 + A_3 x^3\right) \qquad \zeta_1 \le \zeta_m \le \zeta_2 \ , \tag{8}$$

*In practice, the slope of curve A between the origin and ζ_1 is usually selected to yield the correct sonic velocity for low amplitude signals.

where the sum of the A_i coefficients must be unity to guarantee that $\zeta_r(\zeta_2) = \zeta_3$. The quantity x is related to the maximum compression and is expressed as a fraction

$$x(\zeta_m) = \frac{\zeta_m - \zeta_1}{\zeta_2 - \zeta_1} \leq 1 . \tag{9}$$

It is then necessary to require that D lie to the left of C and intersect the ζ axis at ζ_r. If the recovered porosity ($\zeta_r^* - \zeta_r$) is assumed to be restored as a linear function of P, then the following relationship* for α along path D is easily derivable,

$$\frac{1}{\alpha(P)} = \frac{1}{\alpha_c(P)} + \frac{\zeta_r^* - \zeta_r}{P_m} , \tag{10}$$

where α_c is the slope of C at pressure P, and P_m is the pressure corresponding to the maximum compression ζ_m. Since α is determined, the effective bulk modulus k is known and the pressure integration can be accomplished.

The preceding discussion concerned a model for the behavior of microscopic voids normally contained within rock or soil materials. A second type of void must also be taken into account in the pressure calculation. These are voids formed by the opening of cracks in the rock during tensile failure. TENSOR74 does not literally create cracked zones, but it simulates the effect of cracks in a continuum. The occurrence of tensile failure during unloading causes the material to follow a path to the left of the normal unloading path. This behavior is modeled in TENSOR74 by adding a pressure correction δP_t to the pressure when tensile relaxation is occurring. This can happen during both loading and unloading. Similarly, when voids close, a correction δP_c is subtracted. The δP_t calculation will be described in detail when tensile failure is discussed. For now, it will be sufficient to say that δP_t is indicative of the void volume produced by tensile failure. The voids are taken to increase at a rate determined by the bulk modulus k or equivalently the slope α, so that the total void volume is given by

$$\zeta_v = \sum_t \frac{\delta P_t - \delta P_c}{\alpha(P)} . \tag{11}$$

In practice, α is assumed to be approximately constant during tensile failure so that this particular summation is simplified to

*Infinite or negative slopes are not forbidden by Eq. (10). Should such a value be calculated, it is replaced by the slope of a straight line drawn between ζ_m and ζ_r. Although setting the slope to α_c might seem to be more appropriate, such a procedure could cause unintentional bulking by unloading to the left of the origin, depending on the shape of path B.

$$P_v = \sum_t (\delta P_t - \delta P_c) \ , \tag{12}$$

and a "void pressure" P_v is accumulated instead of ζ_t. Void openings from tensile failure add to this summation; void closures subtract.

The net change in pressure during one cycle then consists of three separate contributions

$$\delta P = \alpha \delta\zeta + \delta P_t - \delta P_c \ ,$$

where $\delta\zeta = \rho \dot{\delta} \delta t / \rho_0$ is the incremental volume change. The first term is the simple incrementally elastic contribution. The second term contributes only during tensile failure, and the third term contributes only during loading or reloading provided there are voids.

The form of δP_c during loading must be such that δP is small when P_v or ζ_v is large, allowing the voids to close without resistance. In fact, if the material is not allowed to bulk, δP must be zero until the voids are closed. A form for δP_c which does allow bulking is

$$\delta P_c = \begin{cases} \dfrac{\alpha \delta\zeta}{1 + \alpha\zeta_B / P_v} & \text{loading} \quad (\delta P > 0) \\ 0 & \text{unloading} \quad (\delta P < 0) \ , \end{cases} \tag{13}$$

where ζ_B enters as a characteristic value for the expansion. This form yields the following limits for δP during loading if the δP_t contribution is ignored,

$$\delta P = \begin{cases} 0 & P_v \to \infty \\ e^{-P_v/\alpha\zeta_B} \, \alpha d\zeta & P_v \sim \alpha\zeta_B \\ \alpha d\zeta & P_v \to 0 \ , \end{cases}$$

so that the effect of ζ_B becomes significant when P_v/α is of the order of ζ_B and the correct extreme limits are obtained. The quantity ζ_B is an input parameter to the code and is reset to $\delta\zeta$ if it falls below this value. This artifice allows the void closure to be spread over a minimum of about five time steps in the interest of eliminating numerical noise.

As final comments on the pressure calculation, it should first be noted that no rate-dependent effects are incorporated in the present pressure integration. Secondly, as discussed in the next section, no dilatancy is considered in the present model of shear failure. Should dilatancy be considered at a later date, it could be treated in

somewhat the same fashion as the void volume. Thirdly, the technique for accounting for voids is not unique. Maenchen and Sack[1] in their original version of the TENSOR code accounted for ζ_v directly instead of P_v. Finally, the void closure is independent of the orientation of the tensile failure which produced the voids. The scheme of Maenchen and Sack also took this orientation into account. In future models, their approach or a generalization of it is preferable.

DUCTILE SHEAR FAILURE

The ductile shear failure used in TENSOR74 is essentially an elastic-perfectly plastic model in which the deviatoric state of the material is constrained not to exceed some failure surface. In general, this surface would be a function of stress tensor invariants[7] corresponding to the assumption that the material is initially isotropic. In terms of the stress deviators, three such invariants are

$$P = -I_1/3 = -\frac{1}{3}(T_r + T_z + T_\phi)$$

$$I = I_{2D}^{1/2} = \left(S_r^2 + S_z^2 + S_r S_z + S_{rz}^2\right)^{1/2}$$

$$I_{3D}^{1/3} = \left[(S_r + S_z)\left(S_{rz}^2 - S_r S_z\right)\right]^{1/3} \quad . \tag{14}$$

Data for rock materials indicates that the ductile failure surface can often be adequately described in terms of P and I alone or equivalently P and Y which is defined to be

$$Y = \left(\frac{3}{4} I_{2D}\right)^{1/2}$$

$$= 0.866\ I \quad . \tag{15}$$

Y is proportional to the octahedral shear stress and is equal to the maximum shear stress $(\sigma_1 - \sigma_3)/2$ if σ_2 equals σ_3 as would occur under uniaxial loading.*

However, in the realm of brittle failure (which occurs at lower pressures than ductile failure), compression, extension, and torsion data often cannot be reconciled into a single failure surface by employing only two of the invariants.[3,8] However, the data can often be reduced to a single surface defined in terms of Y and the quantity,

$$\bar{P} = P - \left(\frac{I_{3D}}{16}\right)^{1/3} \quad , \tag{16}$$

*Here, we follow the usual convention in describing the principal stresses: that $\sigma > 0$ in compression, and that $\sigma_3 \leq \sigma_2 \leq \sigma_1$.

which reduces to $\bar{P} = P + Y/3 = (\sigma_1 + \sigma_2)/2$ when σ_2 equals σ_3. In the ductile region, the second term is negligible, so that both brittle and ductile failure surfaces will be described in terms of only Y and $\bar{P}$ as indicated in Fig. 3. The shape of the failure surfaces is similar to that of a modified Prager-Drucker yield criterion.[9] The details of the brittle failure model will be considered in the next section.

In Y-$\bar{P}$ space, material which is shocked will load along a path of slope approximately $(1 - 2\nu)$, corresponding to uniaxial strain loading. If the loading or subsequent reloadings along other paths cause the failure surface to be intersected in the ductile region, the material is said to have experienced ductile failure and the stress state is forced to remain on the failure surface until such time as the stresses subside.

Let us suppose that the integration of the incrementally elastic problem [Eq. (5)] gave solutions $\tilde{S}_r$, $\tilde{S}_z$, and $\tilde{S}_{rz}$ which in turn gave a value $\tilde{Y}$ which lies above the failure surface K at some $\bar{P}$. The final state on the surface is obtained by performing no adjustment on P and by adjusting each of the deviatoric stresses as follows

$$S_i = \tilde{S}_i \frac{K}{\tilde{Y}} \qquad (i = r, z, rz) .$$

This, of course, results in a value of $Y = K$ as desired.

The above stress adjustment, caused by failure, is most certainly accompanied by damage to the material. One measure of the damage is a quantity termed the inelastic or failure-associated strain which is defined as*

$$\begin{aligned} \delta\varepsilon_p &= \frac{1}{2\mu} |\delta I| \\ &= \frac{1}{2\mu} |I - \tilde{I}| \\ &= \frac{\tilde{I}}{2\mu} \left| 1 - \frac{K}{\tilde{Y}} \right| . \end{aligned} \tag{16a}$$

The absolute value is taken because the integral of this quantity is intended to be a measure of the magnitude of incoherent strain experienced by the material,

$$\varepsilon_p = \sum_t \frac{1}{2\mu} \left| I - \frac{K}{\tilde{Y}} \right| .$$

The above formulation for ductile failure does not appear explicitly in TENSOR74. Rather, the ductile problem is formulated as a special case of brittle failure and stress relaxation as discussed below.

*An equivalent parameter differing from this by about 15% could have been defined in terms of Y instead of I.

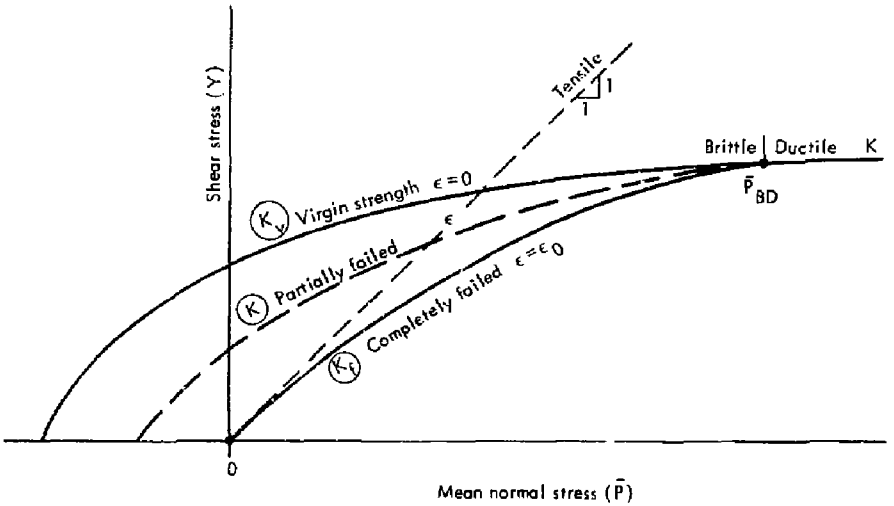

Fig. 3. Shear failure surfaces.

BRITTLE SHEAR FAILURE

The concept of brittle failure employed in TENSOR74 is depicted in Fig. 3 and assumes that the strength of virgin (unfailed) material can be characterized by a curve K_v in Y-$\bar{P}$ space which can be defined by laboratory data, usually triaxial. The unconfined compression test, for example, will define one point along a 45° line from the origin. If the material has tensile strength, K_v will intersect the $\bar{P}$ axis at a negative value of $\bar{P}$. The description of each strength curve is equivalent to a Mohr failure criterion, provided the slope is less than unity.

Further, material that has failed in the brittle mode is assumed to strain soften and to be characterized by a lower strength envelope K that depends on the amount of damage the material has undergone. The damage ε is defined in some fashion analogous to ε_p. In particular, it is assumed that for some limiting value ε_0 of the damage parameter the material has completely failed. It will then possess its lowest possible strength K_f which arises only from the interlocking of the fragments under pressure. Such a material would possess no tensile strength, and K_f should pass through the origin.

A final constraint on K_v, K, and K_f is that they just join at the transition ($\bar{P}_{BD}$) into the ductile region, in effect requiring that there by no sharp discontinuity in the strength descriptions between the brittle and ductile regions. Figure 3 depicts curves satisfying these constraints.

In terms of K_v and K_f, the location of the effective failure surface at a given $\bar{P}$ is taken to be

$$K(\varepsilon) = \begin{cases} K_v - (K_v - K_f)\dfrac{\varepsilon}{\varepsilon_0} & \varepsilon < \varepsilon_0 \\ K_f & \varepsilon \geq \varepsilon_0 \end{cases} , \tag{17}$$

where all quantities are to be evaluated at $\bar{P}$. This form assumes that the effective failure surface is a linear function of ε. Other forms which allow a more gradual onset or termination could certainly be justified.

It is next necessary to describe how the deviatoric stresses are to be relaxed in relation to the effective failure surface K. One option would be to simply "pin" the material to K as in the case of ductile failure. We, however, use a viscoelastic model, which allows some rate dependence to be taken into account. The model used for brittle failure is that of a simple Maxwell solid in shear. This in effect means that stress adjustment behaves as a viscous term in the stress rate Eqs. (5). The form used in the code is

$$S_i = \begin{cases} \tilde{S}_i \left[1 - \frac{\delta t}{\tau}\left(1 - \frac{K}{\tilde{Y}}\right)\right] & \tilde{Y} > K \\ \tilde{S}_i & \tilde{Y} \leq K \end{cases} \qquad (i = r, z, rz) , \tag{18}$$

where δt is the time step. This model produces a damping which increases as $\tilde{Y}$ exceeds K, and which is zero when $\tilde{Y}$ and K coincide. The quantity τ, called the Maxwell relaxation time, is the characteristic time over which the stress relaxation is to take place.

It should be noted that if τ is taken to be δt, then this equation reduces to the relaxation equation for ductile failure. Accordingly, it is possible to develop an artifice which allows the unified treatment of both brittle and ductile relaxation. This is accomplished by defining,

$$\tau = \begin{cases} \tau_0[1 - (K_f/K_v)] \\ \delta t \text{ as a lower bound} , \end{cases} \tag{19}$$

where τ_0 is the input relaxation time. This relation produces an effective relaxation time which reduces to δt in the ductile region, which is τ_0 when $K_f = 0$, and which possesses a smooth transition between the two limits.

The net effect of the above formulation [Eq. (19)] is to allow Y to overshoot the failure surface K in the brittle region under rapid loading conditions (thus producing a "rate hardening"), and to gradually force the overshoot to vanish as the ductile transition is approached. This is done in the interests of using an elastic-perfectly plastic model *of ductile flow. It may well be that rate dependence in the ductile region* is also desirable, in which case Eq. (19) should be modified or discarded.

We need finally to fully specify the calculation of the failure associated strain ε for all shear failure.

$$\delta\varepsilon = \frac{1}{2\mu} |\delta I| = \frac{\delta t}{2\mu\tau} \tilde{I}\left|1 - \frac{K}{\tilde{Y}}\right| , \tag{20}$$

which is consistent with $\delta\varepsilon_p$ as defined for the ductile region [Eq. (16a)] when $\tau = \delta t$.

The shear failure model as described above does not take into account shear-volume interactions (dilatancy and shear enhanced compaction). This would require a flow rule that adjusts P as well as Y. Once such a flow rule is adequately defined, it can be incorporated in the code in much the same manner as is the δP_t adjustment described below. The current model also neglects ductile strain hardening in which the strength increases with the strain.

TENSILE FAILURE

Tensile relaxation is described in the principal stress coordinate system (in which the off-diagonal component T_{12} vanishes). This system is obtained by a rotation in the r-z plane of

$$\psi = \frac{1}{2} \text{Tan}^{-1} \left(\frac{2S_{rz}}{S_z - S_r} \right) ,$$

which results in principal stresses* of

$$\left.\begin{matrix} T_1 \\ T_2 \end{matrix}\right\} = -P + \frac{1}{2}\left\{ S_r + S_z \pm \left[(S_r - S_z)^2 + (2S_{rz})^2 \right]^{1/2} \right\}$$

$$T_3 = -P - S_r - S_z . \qquad (21)$$

If any of these are positive, the material is in tension. T_3 is always in the ϕ direction and is commonly referred to as the hoop stress. As $T_1 > T_2$ by definition, T_2 is the most compressive of the two and is directed perpendicular to the shock front. T_1 is the maximum principal stress in the r-z plane but may be less than T_3 and, by default, lies parallel to the shock front in compressive shock loading. The tensile states typically encountered are those in which two of the principal stresses are tensile and the third is compressive. In Y-$\bar{P}$ space, these states lie to the left of the dashed line of unity slope depicted in Fig. 3.

In the code, the criterion for initiation of tensile failure is taken to be the same as that for shear failure, although the relaxation technique is different. This unified shear-tensile failure criterion corresponds to the notion that tensile failure must be preceded by the creation of cracks by large stress deviators. Once a crack has occurred for any reason, it is then free to open if there is tension. Along with the opening of the crack, tensile stress relaxation occurs. All principal stresses which are tensile are allowed to relax. Unlike shear failure, in which the material strength is gradually reduced to zero, the material behaves under tensile failure as if its tensile strength has been instantaneously set to zero when the failure surface is first reached. Alternatives to this approach are discussed later.

The relaxation model for tensile failure is again taken to be a Maxwell solid, so that the tensile principal stresses are adjusted as follows:

---

*The convention followed in defining ψ is not identical to that of [illegible]. Here, T_1 [illegible] is tension, and $T_1 \geq T_2$, and T_3 lies in the ϕ direction.

$$T_i = \begin{cases} \tilde{T}_i \left(1 - \frac{\delta t}{\tau}\right) & \tilde{T}_i > 0 \\ \tilde{T}_i & \tilde{T}_i < 0 \end{cases} \qquad (i = 1, 2, 3) \qquad (22)$$

in which the tilde indicates the old value from Eq. (21). Usually τ is very close to τ_0 [Eq. (19)] because most tension occurs near $\bar{P} = 0$ at which $K_f = 0$. The relaxation time for tension and shear have been taken to be the same for lack of compelling reasons why they should not be.

It is next necessary to find the new values of S_r, S_z, and S_{rz} corresponding to the tensile-relaxed principal stresses. If it is assumed that the opening of tensile cracks as modeled by the above relaxation does not rotate the principal coordinate system, then the transformation Eqs. (21) can be inverted to yield,

$$\left.\begin{matrix} S_r \\ S_z \end{matrix}\right\} = \bar{P} + \left(\frac{T_1 + T_2}{2}\right) \pm \left(\frac{T_1 - T_2}{2}\right) \cos 2\psi$$

$$S_{rz} = \left(\frac{T_1 - T_2}{2}\right) \sin 2\psi \ .$$

During the relaxation, the trace of the stress tensor is altered, so that the pressure and other invariants must also be adjusted. The expression for the pressure correction is

$$\begin{aligned} \delta P_t &= \bar{P} - \tilde{\bar{P}} \\ &= \frac{1}{3} \sum_i \delta T_i \ , \end{aligned} \qquad (23)$$

where δT_i is the amount by which each of the tensions was adjusted. This is the final correction to the pressure calculation.

Because tensile failure also alters the second deviatoric invariant, the final step in the tensile failure scheme is to increment the accumulated damage. In addition, we add a term which represents the volumetric strain associated with crack opening. Thus,

$$\delta\epsilon = \frac{1}{2\mu} |\delta I| + \frac{1}{K} |\delta P_t| \ , \qquad (24)$$

where each term is determined by comparing the old and new values for I or P_t, respectively.

The foregoing has been a description of the primary tensile failure model used in HASS0174. The model is intended to be a isotropic continuum model and consequently describes incoherent breakage. That is, the planes of separation or fracture are assumed to be randomly oriented. Such a model is easily defensible in a one-dimensional code,

however, the desirability of an isotropic model in a two-dimensional code is questionable because tensile failure should include anisotropy via aligned cracks. For example, suppose $T_3 > T_1$, and that T_3 is primarily responsible for driving the material to failure. Intuitively, one would expect that the fracture plane would be perpendicular to T_3. A description of this phenomenon would require that T_3 be allowed to relax, and that the material maintain its strength in the T_1 direction. One way to achieve such an effect would be to test each tensile principle stress independently against a single tensile strength limit. Only those tensions exceeding the limit would then be relaxed. Once tensile failure occurs in a given direction, the strength in that direction is allowed to drop to zero either gradually or immediately. Such a model was employed by Maenchen and Sack[1] in their original version of the TENSOR code.

An alternative method which preserves the unified shear-tensile failure criterion was formulated in a special version of TENSOR74.* In this model, two tensile relaxation schemes were employed.

$$T_i = \tilde{T}_i\left(. - \frac{\delta t}{\tau}\right) \qquad \text{(rapid relaxation)},$$

or

$$T_i = \tilde{T}_i\left(1 - \frac{\delta t}{\tau}\frac{\epsilon}{\epsilon_0}\right) \qquad \text{(slow relaxation)} . \qquad (25)$$

The second equation has an effective relaxation time of $\tau\epsilon_0/\epsilon$ which is large until the material is heavily damaged. As in the previous model, the maximum principal stress which is responsible for failure (say, T_3) would be allowed to relax rapidly according to the first relation. T_1 would follow the second relation in Eq. (25) and would relax slowly or rapidly according to the extent to which the material is damaged. Because of the rapid relaxation of T_3 relative to T_1 it may well be that after a few cycles their roles are reversed ($T_1 > T_3$). This situation is handled in the following manner: If Y exceeds the effective failure surface K at any given time, the most tensile stress at that time is flagged and assigned the rapid relaxation in addition to any other stresses which may have been previously flagged. In this way, both T_3 and T_1 can be relaxed quickly if each was at one time or another the tensile stress which drove the material above the failure surface. This scheme takes coherent failure into account but allows the possibility of incoherent relaxation at large damage levels.

Both this scheme and the one of Maenchen and Sack suffer a serious flaw. The true planes of failure should be fixed in the material coordinates. In both of these schemes, the planes are fixed instead in the principal coordinate system which is free to rotate with respect to the material as the applied stresses vary with time. This problem is especially acute when several energy sources are involved or when reflecting surfaces are present.

*The version TEN51B has been used extensively in a study of the blasting effects of long cylindrical charges.[10,11]

Another serious flaw in the tensile failure models discussed above is that, unlike the shear failure model, the material tensile strength is immediately set to zero on failure. Because of this discontinuous alteration in behavior, the first zone in a region to fail may be relaxed before adjacent zones are stressed to failure. This apparently leads to the propagation of finger-like regions of failure which resemble fracture planes.[10,11] While there is some physical reality to these propagating disturbances, it would be imprudent to place much credence in them without more study. For the present, it would perhaps be more desirable to follow the shear failure procedure and let the tensile strength be gradually reduced to zero depending on the damage parameter. A model which properly solves both the isotropy problem and the tensile strength problem might involve the replacement of the damage parameter by an inelastic strain tensor. Both the shear and tensile relaxation rates could then be governed by the extent of damage in the appropriate direction. The relaxation, in turn, would produce inelastic strain which would be added to the proper components of the inelastic strain tensor.

ARTIFICIAL VISCOSITY, STABILITY, ENERGY

Artificial viscosities are used to damp out spurious oscillations. In all, six such terms which depend on three input coefficients C_i and one width W are used in HENSOR74. Four of the six viscosity terms are Q, Q_r, Q_z, and Q_{rz} which are added respectively to P, T_r, T_z, and T_{rz} in both the momentum equations [Eq. (3)] and also in the internal energy equation, which is discussed later in this section.

The viscosity Q applied to the pressure is a sum of two terms, a quadratic and a volumetric viscosity.

$$Q = C_1\rho(\Delta u)^2 - \rho c l \dot{\delta} \ . \tag{26}$$

The first or quadratic term is a "standard" Von Neumann[12] term discussed by Schatz[3] and is proportional to the square of the velocity difference Δu across the zone. If the zone is expanding, Δu is set to zero.

For shock loading or one-dimensional loading, the second term can be properly referred to as a linear viscosity* except very near the origin or axis of symmetry. Unlike the quadratic term, this term is always used independent of the sign of $\dot{\delta}$. The characteristic length l has been found to produce a shock width of about five zones when

---

*The code user also has the option of using a conventional linear viscosity instead of the volumetric viscosity,

$$Q(\text{linear}) = C_4\rho c\sqrt{(\Delta u)^2} \ .$$

As with the quadratic term, Δu is set to zero if the zone is expanding. If this option is used, C_4 replaces the quantity $l/6\dot{\delta}$ in the stability Eq. (28).

L is about one-tenth of the zone size.[3] This relationship enables the code user to select the shock width W, usually taken to be about five zone sizes. The input width is then converted to L = W/50 internally. This form for the linear viscosity has the property of damping the motion of both contracting and expanding zones, an advantage in spherical shock expansion problems, but a disadvantage in spall calculations. Spall, which involves the free expansion of zones near the surface, cannot be modeled accurately unless the viscous terms are negligible during expansion. In this case the optional conventional linear artificial viscosity should be used.

The deviatoric viscosities are determined from

$$Q_i = C_2 \rho c L \frac{2\mu}{\alpha} e_i \qquad (i = r, z, rz) \ . \tag{27}$$

The ratio $2\mu/\alpha$ is intended to produce greater damping for highly compressible materials or for those with a high shear modulus.

The final two viscosity terms q_r and q_z are added, respectively, to the two momentum equations [Eq. (3)] to control "hourglass" distortion. This is a type of oscillation in which the zone diagonals are translated in opposite directions. This oscillation arises because the numerical expressions for the strain rates are unaffected by this type of distortion. Consequently, the artificial viscosities previously discussed will not damp this mode of oscillation. As this is purely numerical phenomenon, expressions for q_r and q_z, which depend on a coefficient C_3, will not be given here. Reference 2 contains a complete discussion.

The artificial viscosities affect the time step through a stability criterion,

$$\delta t = \frac{C_0 \delta D}{\left[c^2 + 4c^2\left(\frac{L}{\delta D}\right)^2 + 4C_1^2(\Delta u)^2\right]^{1/2}} \ . \tag{28}$$

This quantity is calculated for each zone, and the smallest δt found throughout the mesh is used as the time step for the next iteration. C_0 is the Courant number and δD is a number which is approximately the smallest zone dimension. Equation (28) is a generalization of the stability condition proposed by Von Neumann and Richtmyer.[12] If the first term under the radical is considered alone, Eq. (28) represents the stability condition for the pure hydrodynamic (hyperbolic) equation. The last two terms correspond to the volumetric and quadratic viscosities, respectively, and force Eq. (28) to represent the stability condition for the diffusion equation. This is done because the equations of motion [Eq. (3)] reduce to a diffusion (parabolic) equation in the limit of large viscosities. The stability requirements corresponding to the brittle and ductile relaxation schemes are not presently reflected in the stability calculation.

TENSOR74 problems are often discretized so that small zones are near the energy source. The zoning is then graded to larger zone sizes near the periphery of the problem. This is usually done in an effort to simultaneously obtain solutions to both

a finely zoned close-in problem and a coarsely zoned far-out problem. The form of the volumetric viscosity, however, works against such an approach. First, for the solution to be stable when the shock reaches the larger zones, L (or equivalently W) must be chosen to correspond to the size of the larger zones. This means that the problem is highly overdamped in the region of the small zones where the shock originates, resulting in much smaller initial time steps than necessary.

The above problem does not arise in hydrodynamics codes using a conventional linear viscosity formulation[3] because L is in effect chosen for each zone by keeping $C_4 \sim L/\delta D$ constant. In problems with nonuniform zoning, there may be large systematic variations in the zone size between two regions at the same distance from the source. For such problems, the variation in artificial viscosity resulting from a conventional formulation can result in systematic motions which may be easily confused with a true problem solution. The elimination of spurious zoning effects such as this is one of the primary advantages of the viscosity formulation used in TENSOR74.

There exists a compromise between the two methods which is worthy of further consideration. This involves simply forcing the code to choose L based upon the largest zone which is active at a given time. In this way, all zones experience the same damping at the same time. As the shock wave moves outward, activating more zones, the viscosity then increases everywhere as required to give a stable solution for the larger zones.

Finally, the internal energy equation

$$\dot{E} = -P\dot{V} + (2S_r + S_z)\dot{e}_r + (2S_z + S_r)\dot{e}_z + 2S_{rz}\dot{e}_{rz} \tag{29}$$

is integrated to arrive at the new internal energy (per original unit volume) for each zone. As indicated earlier, the appropriate viscosities are added to each stress in Eq. (29) before the integration.

FUTURE WORK

Much work remains to be done in the rock mechanics modeling of TENSOR74. In the near future, we hope to examine the question of anisotropy and its modeling with respect to shear and tensile strength and relaxation, damage, and void closure. The desirability of the present unified shear-tensile failure will also be questioned. In connection with the relaxation schemes, it will be necessary to examine their effect on stability. The effect of shear stress on the compaction of porous material will also be modeled.

We plan to formulate a new artificial viscosity tensor in the coordinate system of the principal strain rates. This will replace the present formulation — Eqs. (26) and (27).

In the area of general code development, we plan to improve the convergence rate of the existing quasi-static mode of operation, to reexamine the present gravity and overburden formulations, and to develop new nonreflecting boundary conditions.

REFERENCES

1. G. Maenchen and S. Sack, The TENSOR Code, Lawrence Livermore Laboratory, Rept. UCRL-7216 (1963).
2. J. T. Cherry, S. Sack, G. Maenchen, and V. Kransky, Two-Dimensional Stress-Induced Adiabatic Flow, Lawrence Livermore Laboratory, Rept. UCRL-50987 (1970).
3. J. F. Schatz, SOC73, An Improved One-Dimensional Wave Propagation Code for Rock Media, Lawrence Livermore Laboratory, Rept. UCRL-51689 (1974).
4. W. Prager, Introduction to Mechanics of Continua (Ginn and Co., Boston, 1961), Chapt. 8.
5. J. Hannon, Lawrence Livermore Laboratory, private communication (January 1974).
6. R. Terhune, D. Stephens, and F. Petersen, Lawrence Livermore Laboratory, Internal Document UOPKL-72-46 (1972). Readers outside the Laboratory who desire further information on LLL internal documents should address their inquiries to the Technical Information Department, Lawrence Livermore Laboratory, Livermore, California 94550.
7. J. White, An Invariant Description of Failure for an Isotropic Medium, Lawrence Livermore Laboratory, Rept. UCRL-72065, Rev. 2 (1972).
8. J. T. Cherry and F. L. Petersen, Numerical Simulation of Stress Wave Propagation from Underground Nuclear Explosions, Lawrence Livermore Laboratory, Rept. UCRL-72216 (1970).
9. J. Isenberg, Nuclear Geophysics, Part II: Mechanical Properties of Earth Materials, Agbabian Associates, El Segundo, CA, Rept. DNA 1285H2, November 1972.
10. C. M. Snell, M. Heusinkveld, J. Bryan, and D. Burton, Progress Report: Controlled Blasting Calculational Studies, Lawrence Livermore Laboratory, Rept. UCID-16551 (1974).
11. M. Heusinkveld, J. Bryan, D. Burton, and C. M. Snell, Controlled Blasting Calculations with the TENSOR74 Code, Lawrence Livermore Laboratory, Rept. UCRL-51740 (1975).
12. J. Von Neumann and R. D. Richtmyer, J. Appl. Phys. 21, 232 (1950).

MBB/lt